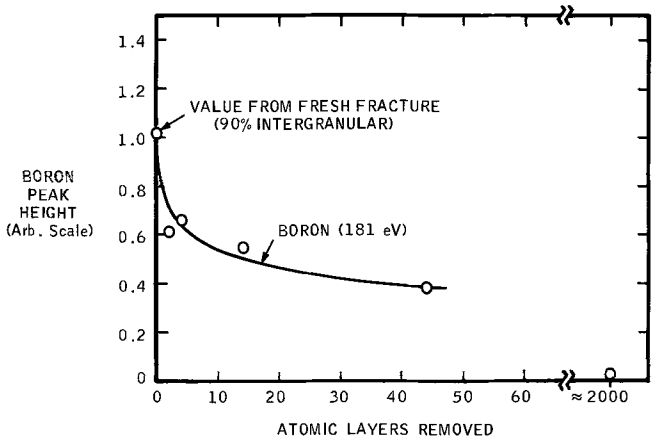

Fig. 2—Boron concentration profile in terms of boron (181 eV) peak height *vs* atomic layers removed by argon ion sputtering.

ular facets was obtained by determining the boron concentration profile, *i.e.*, the Auger boron peak height as a function of depth beneath the fracture surface. The profile, presented in Fig. 2, was obtained by controlled sputtering (by argon ion bombardment) of material from the fracture surface in small steps and performing Auger analysis for boron at each step. The rapid decrease in boron concentration in the first 10 atomic layers, followed by a more gradual decrease out to approximately 2000 atomic layers suggests the presence of both equilibrium segregation (Gibbsian adsorption) and nonequilibrium segregation (from diffusion of vacancy/boron complexes to grain boundaries during cooling from high temperatures). The fact that the strong molybdenum Auger peak at 183 eV [3] was not detected, indicated that molybdenum was not segregated at the grain boundaries.

In summary, the present communication reports the observation of two positions for the principal Auger peak for boron, one at 181 eV for elemental boron, and one at 170 eV for boron chemically bound in a phase commonly found in boron steels, $Fe_{23}(C, B)_6$. While this chemical shift of the Auger boron peak and similar shifts reported for Al, Ta and Si are of general scientific interest, the present observation regarding elemental boron carries special metallurgical significance because it appears to be the first direct evidence for segregation of atomic boron at grain boundaries in steel. The door is now open for the application of Auger electron spectroscopy to the study of grain boundary segregation of boron in steel, hopefully leading to an understanding of the respective effects of atomic boron and of precipitated boron-containing phases in two important areas of steel metallurgy—hardenability and grain boundary embrittlement.

1. D. F. Stein, A. Joshi, and R. P. Laforce: *Trans. ASM,* 1969, vol. 62, pp. 776-83.
2. L. A. Harris: *J. Appl. Phys.*, 1968, vol. 39, pp. 1419-27.
3. *Handbook of Auger Electron Spectroscopy,* published by Physical Electronics Industries, Inc., Edina, Minnesota.
4. H. E. Bishop and J. C. Riviere: *Acta Met.*, 1970, vol. 18, pp. 813-17.
5. Ph. Maitrepierre: Institut de Recherches de la Siderurgie Francaise (IRSID) Saint-Germain-en-Laye, France, unpublished research, 1974.
6. J. B. Lumsden III: The Ohio State University, Corrosion Center, Department of Metallurgical Engineering, Columbus, Ohio, unpublished research, 1974.
7. T. W. Haas and J. T. Grant: *Phys. Lett.*, 1969, vol. 30A, p. 272.
8. P. W. Palmberg: Proceedings Electron Spectroscopy Conference, D. A. Shirley, ed., p. 845, Asilomar, California, 1972.

Plastic Zone Sizes in Fatigued Specimens of INCO 718

M. CLAVEL, D. FOURNIER, AND A. PINEAU

The size of the plastic zone at the head of a fatigue crack is an important parameter in the discussion of fatigue crack growth behavior. In his theoretical model, Rice showed that a reversed plastic zone is present within the so-called monotonic plastic zone when the material is stress-cycled.[1] His calculations indicate that the size of the reversed plastic zone is one fourth that of the monotonic one. Various experimental approaches such as X-ray microbeam studies,[2] etching technique in Fe-3 Si[3] and microhardness measurements[4-5] have been used to measure plastic zone sizes. The etching technique in Fe-3 Si and the microhardness measurements in austenitic and martensitic steels showed the presence of a reversed flow within the monotonic plastic zone as predicted by Rice.[1]

The microhardness technique is best suited, however, to materials which are cyclically unstable, *i.e.* which strongly work-harden like austenitic stainless steels or which strongly work-soften like maraging steels. In the work reported here, we have developed an etching technique which can be used for INCO 718. This alloy which is almost cyclically stable is not easily amenable to the microhardness technique.

INCO 718 is strengthened mainly by γ'' (DO_{22}) and also by γ' ($L1_2$) precipitates.[6] Kirman and Warrington showed that room temperature deformation of a γ'' dispersion produces faults within the γ'' precipitates.[7] These faults can give locally the stacking sequence *ABAB* which is that of the stable orthorhombic (DO_a) β phase. During further aging of the alloy these strain-induced defects act as nuclei for the β phase which then grows as long platelets on the (111) planes of the matrix. After this post-deformation aging treatment, the β phase can be easily observed by either optical or scanning electron microscopy. Observations on fully-aged tensile specimens showed that a heat-treatment (943 K for 80 h) was sufficient to evidence plastic strains less than about 1 pct.

In measurements of the plastic zone size during fatigue crack propagation two types of conventional fatigue specimens were used, CT and SEN. The dimensions of the specimens are given in Figs. 1(*b*) and 1(*c*). The SEN and CT specimens were fatigued at high and low load levels, respectively. For the SEN specimens a maximum load of 25.5×10^3 N was used, while the CT specimens were fatigue tested at 4.91×10^3 N maximum load. In both cases the ratio between the minimum and the maximum load, R, was 0.10. In order to eliminate any effects of plastic flow around the machined notch during crack initiation, measurements of zone sizes were only begun after 10^{-3} m of fatigue crack growth. Measurements were made both at the surface (plane stress) and at the midplane of the specimens (plane strain). On the surface the plastic zone size determined by this etching technique was com-

M. CLAVEL, D. FOURNIER, and A. PINEAU are with the Centre des Materiaux of Ecole des Mines de Paris.

Manuscript submitted May 23, 1975.

pared with the size of the deformation zone which could be directly observed before post-deformation aging.

The specimens were annealed at 1228 K for 30 min and fully aged (993 K-8 h—air cooling at 50 K/h to 893 K-8 h). This conventional heat-treatment gave a grain size of about $40 \cdot 10^{-6}$ m and a yield strength at 0.2 pct (σ_y) of 1070 MPa.

The crack growth rates measurements (da/dN) *vs* the variation of the stress intensity factor (ΔK) are plotted in Fig. 1(*a*). It should be noted that the results obtained with the two types of specimens are very close together in the range of ΔK common to both tests.

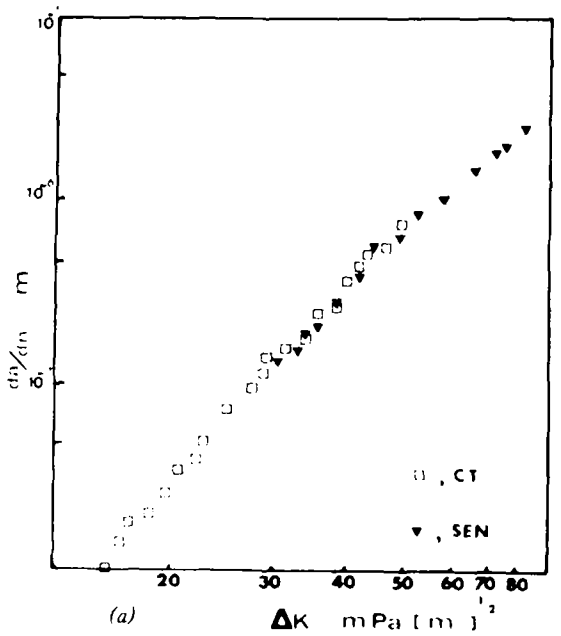

(*a*)

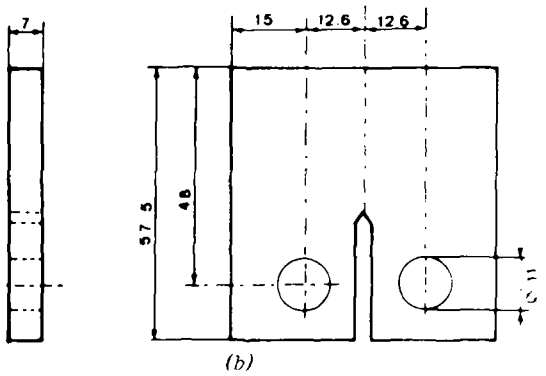

(*b*)

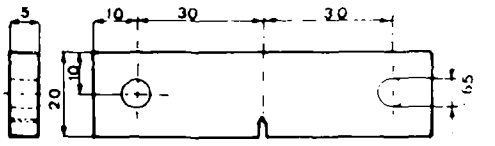

(*c*)

Fig. 1—(*a*) Crack growth rates (da/dN) *vs* the variation of the stress intensity factor (ΔK). Results obtained with the CT and SEN specimens are included. (*b*) and (*c*) CT and SEN specimens, respectively. (All dimensions are given in mm).

Fig. 2—Plastic zone attending a fatigue crack decorated by β platelets and observed by scanning electron microscopy. Mid-plane of a SEN specimen fatigued at ΔK = 55 MPa $\sqrt{m}$ (Rp = $24 \cdot 10^{-5}$ m). The extent of the monotonic plastic zone revealed by the intergranular precipitation of β platelets is indicated by a dotted line.

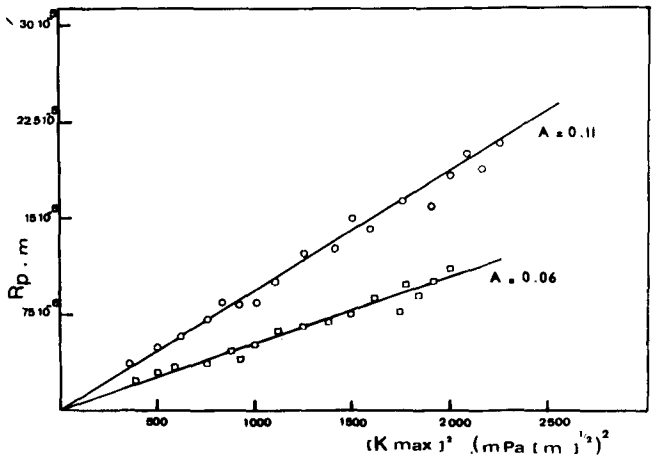

Fig. 3—Measurements of the monotonic plastic zone sizes of CT specimens. The results for plane stress (upper curve) and plane strain (lower curve) conditions are given. The A coefficients were calculated with σ_y = 1070 MPa.

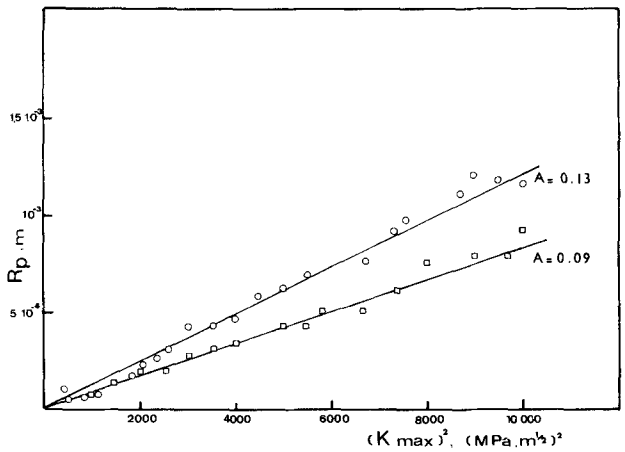

Fig. 4—Variation of the monotonic plastic zone sizes of SEN specimens with Kmax. The results for plane stress (upper curve) and plane strain (lower curve) conditions are included. The A coefficients were calculated with σ_y = 1070 MPa.

Fig. 2 shows an example of the decoration by β platelets of the plastic zone attending a fatigue crack. It can be noted that the presence of the β phase within the grains is restricted to a zone below the fracture surface. In the regions which were not deformed, the precipitation of the orthorhombic phase occurs only at the grain boundaries. Inside the plastic zone, the density of β platelets increases continuously from the elastoplastic boundary or the monotonic zone interface to the fracture surface. It is not possible to determine the limit of the reversed zone by this etching technique. Moreover the accuracy of this etching technique to delineate the plastic zones is thought to be of the order of the grain size, *i.e.* $\pm 20 \cdot 10^{-6}$ m.

The monotonic plastic zone size (R_p) was measured on various specimens and for various crack lengths in order to study a large range of ΔK. The results for CT and SEN specimens are given in Figs. 3 and 4, respectively. In both cases results for plane strain and plane stress measurements are included. The surface measurements were found to be in good agreement with those observed from deformation zone. The plastic zone sizes are plotted *vs* $(K_{\max})2$, where $K_{\max}$ is the maximum of the stress-intensity factor. The monotonic plastic zone is thought to be best correlated with $K_{\max}$ rather than ΔK.

The results show that the Irwin's relationship, $R_p = A \times (K/\sigma_y)^2$ for monotonic plastic flow is verified. The plane strain plastic zone is approximately half the plane stress plastic zone. This ratio is larger than that predicted by the Irwin's model which gives a factor of 1/3. In plane strain conditions, the difference in the A coefficients between CT and SEN specimens is not considered to be significant because the measurements were not performed in the same K range for the two types of specimens. The A coefficient for plane strain conditions is very close to that found by microhardness measurements in CT specimens,[4,5] but is smaller than that determined by Hahn *et al*[3] in DCB specimens of Fe-3 Si. Moreover, the A coefficients reported here are very close to the theoretical value $(1/3\pi)$ calculated by Irwin.

In summary, this etching technique is suitable to measure the plastic zone sizes in INCO 718. It is currently being used in a study of the fatigue behavior of this alloy. Since this method is specific to the $\gamma'' \rightarrow \beta$ phase transformation it can also be used for INCO 706 which is also strengthened by γ''.[8,9] The same principle of post-deformation heat-treatment to delineate plastic zones could be used, for instance, in Fe-Ni-Cr-Ti alloys which exhibit a strain-accelerated $\gamma' \rightarrow \eta$ (DO_{24}) transformation.

1. J. R. Rice: ASTM Spec. Tech. Publ. 415, p. 247, American Society for Testing and Materials, 1967.
2. T. Matsumoto and H. Kitagawa: *Proc. of the Int. Conf. on Mech. Behavior of Materials, 1971*, vol. 2, p. 59. The Society of Materials Science, Japan, 1972.
3. G. T. Hahn, R. G. Hoagland, and A. R. Rosenfield: *Met. Trans.*, 1972, vol. 3, p. 1189.
4. C. Bathias and R. Pelloux: *Met. Trans.*, 1973, vol. 4, p. 1265.
5. A. Pineau and R. M. Pelloux: *Met. Trans.*, 1974, vol. 5, p. 1103.
6. D. F. Paulonis, J. M. Oblak and D. S. Duvall: *Trans. ASM*, 1969, vol. 62, p. 611.
7. I. Kirman and D. H. Warrington: *Met. Trans.*, 1970, vol. 1, p. 2667.
8. J. H. Moll, G. N. Maniar, and D. R. Muzyka: *Met. Trans.*, 1971, vol. 2, p. 2143.
9. R. Cozar and A. Pineau: *Met. Trans.*, 1973, vol. 4, p. 47.

Effect of Plastic Strain on the r Value of Textured Steel Sheet

HSUN HU

It was shown previously[1] that the r_m values of deep-drawing sheet steels are highly strain-dependent within the range of uniform deformation in a simple tension test. Based on an analysis of the work hardening rate in the thickness and in the width dimensions of the specimen, which differed considerably as a consequence of texture strengthening, it was anticipated that whereas the r value for strongly (111)-textured sheet ($r > 1.00$) decreases with increasing strain, the r value for random-textured sheet ($r \simeq 1.00$) should be independent of strain, and that for strongly (100)-tex-

HSUN HU is Staff Scientist, Research Laboratory, U.S. Steel Corporation, Monroeville, Pa. 15146.

Manuscript submitted May 23, 1975.